Journal of Engineering Physics and Thermophysics, Vol. 76, No. 2, 2003

SUPERDEEP PENETRATION

S. K. Andilevko

UDC 534.2

The theoretical foundations of the effect of superdeep penetration are considered, a concrete case of loading of an obstacle by a powder flux is calculated, and the calculation data are compared with the available results of a nature experiment.

The superdeep-penetration effect discovered approximately 25 years ago immediately came to the attention of researchers [1–9], but till now it has not been exhaustively explained from the viewpoint of the theory of interaction of solid bodies. A description of the experimental results of numerous investigations carried out by different groups of scientists is given in [10]. In the present paper, the theoretical aspects of this phenomenon are described.

Necessary Condition of Superdeep Penetration. Virtually all researchers studying superdeep penetration [1–7, 9] arrive at the conclusion that the material near the penetrating particles must be made softer locally. To do this, the energy of interaction of a particle with the material of the obstacle must be concentrated in the slip plane where this particle moves; otherwise it will be jammed in the near-surface layers of the obstacle without overcoming the distance $\sim d$. To implement this softening, it is necessary that the characteristic time of interaction $\tau_{int} = d/U$ be not longer than the time it takes for the energy to be removed from the zone of interaction by the thermal mechanism $\tau_{th} = \Delta^2/a$. The relation obtained

$$\frac{d}{U} \le \frac{\Delta^2}{a}, \quad \text{or} \quad d \le d_{\lim} = \frac{\Delta^2 U}{a}, \tag{1}$$

is the necessary condition of occurrence of superdeep penetration, which was formulated for the first time in [1]. It sets the limiting size of the penetrating particles $d_{\lim}$. Particles with $d > d_{\lim}$ cannot penetrate into the obstacle. However, as is proved in [3], the fulfillment of (1) is inadequate to implement superdeep penetration.

Sufficient Condition of Superdeep Penetration. After the collision with the surface of the obstacle, the flux particles continue to move in the metal that has already lost its strength if condition (1) is fulfilled. At the initial stage of their motion, the velocity of the particles decreases rapidly. This continues until the depth of penetration of the particles h exceeds d. Let us consider the motion of a particle at depth $h \ge d$ on condition that the action of the particle flux produces the field of the pressure p in the obstacle. We assume that over a physically short time interval Δt the process can be approximated using the representations of stationary flow of a viscous fluid around a particle. We use the results obtained in [11] on calculation of the drag force in the case of stationary flow of a viscous fluid around a body of arbitrary shape. The component of this force in the direction of flow F_x is equal to

$$F_x = -\rho U \int_{\Delta S} v_x dy dz, \tag{2}$$

where x coincides with the direction of motion of the particle (striker), and y and z are perpendicular to it. The integration is made over the area of the cross section ΔS of the wake which is formed by the particle and is separated from its back surface by a large distance. Here U is the constant velocity of the viscous fluid flow incident on the body, and the true velocity of the fluid at each point will be $U + v$, where $v << U$. At infinity, v becomes zero. Evidently, the drag force depends directly on the cross-sectional area of the wake formed by the striker in the fluid. In

A. V. Luikov Heat and Mass Transfer Institute, National Academy of Sciences of Belarus, Minsk, Belarus. Translated from Inzhenerno-Fizicheskii Zhurnal, Vol. 76, No. 2, pp. 12–18, March–April, 2003. Original article submitted October 21, 2002.

 1062-0125/03/7602-0242$25.00 ©2003 Plenum Publishing Corporation

this case (we will assume for the sake of definiteness that the particle has a spherical shape), this wake is a channel formed by the particle moving in the obstacle. However, as a result of the action of the particle flux on the surface of the obstacle, in it there arises the field of the pressure p under which the cross section of the wake significantly decreases. In the limit, if the channel in the wake of the particle closes completely, $\Delta S \to 0$ and the integral in (2) also tends to zero. In this case, the particle moves uniformly without meeting resistance from the fluid. This is possible if the time of complete closing of the channel τ_{cl} does not exceed τ_{int}. The spherical particle, moving in the material, forms a cylindrical channel. The time it takes the channel to close can be determined from the system of equations for the one-dimensional case with axial symmetry [12]:

$$\frac{\partial u}{\partial t} + u\frac{\partial u}{\partial r} = -\frac{1}{\rho}\frac{\partial p}{\partial r}, \quad \frac{\partial \rho}{\partial t} + \frac{\partial (\rho u)}{\partial r} + \frac{\rho u}{r} = 0, \quad p = p(\rho, T). \tag{3}$$

The last expression in (3) is the equation of state of the obstacle material. Let us assume that the pressure in the obstacle changes relatively slowly in comparison with τ_{int}. Then, it may be logically assumed that the radial velocity component of the medium also depends weakly on time, $\partial u/\partial t = 0$. At pressures of ~10 GPa realized in the case of superdeep penetration, the compressibility of a metal manifests itself insignificantly; therefore, instead of the second equation of (3), we obtain

$$\frac{\partial u}{\partial r} = -\frac{u}{r}. \tag{4}$$

Having substituted (4) into the first equation of (3), we will have $-\frac{u^2}{r} = \frac{1}{\rho}\frac{\partial p}{\partial r}$. Replacing the pressure gradient by its average value $-2p/d$, in the first approximation we obtain

$$u = -\sqrt{\frac{2pr}{d\rho}}. \tag{5}$$

By definition, $u = dr/dt$. Substituting this quantity into (5), we arrive at the differential equation

$$\frac{dr}{dt} = -\sqrt{r}\sqrt{\frac{2p}{d\rho}}. \tag{6}$$

Integration of (6) with the conditions $r(t = 0) = d/2$ and $r(t = \tau_{cl}) = 0$ gives

$$\tau_{cl} = \sqrt{\frac{\rho d^2}{p}}. \tag{7}$$

The fact that the channel must close over a period of time shorter than the characteristic time of interaction τ_{int} yields

$$U_p \le U_{max} = \sqrt{\frac{p}{\rho}}. \tag{8}$$

In its meaning, (8) is a sufficient condition of superdeep penetration. If it is not fulfilled, a particle will be intensely retarded in the obstacle until its velocity is equal to U_{max}. Once $U_p = U_{max}$, or $U_p \le U_{max}$ initially, the motion of an object in the obstacle material will be uniform if we disregard the random processes of its collisions with inclusions and inhomogeneities, characteristic of any actual metal. An unusual kind of analog of the classical D'Alembert paradox [11, 12] occurring in a perfect fluid is realized. It can be realized in the case considered (the softened obstacle material differs greatly from a perfect fluid in its properties), because the external energy source (partial flux) does a certain work and supplies the obstacle with an energy dissipating in it and providing the closing of the channels in the wake of the penetrating particles, which permits them to move in the obstacle material without meeting resistance. The assumption that the D'Alembert effect is responsible for superdeep penetration was made for the first time in [1].

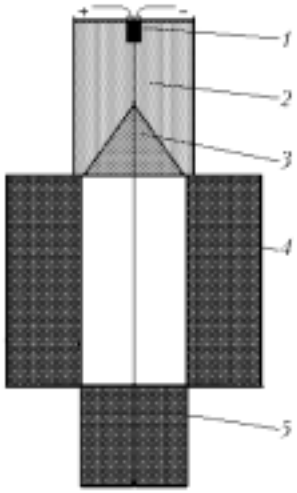

Fig. 1. Diagram of the accelerator of powder particles, used in the experiments on superdeep penetration in [16, 17]: 1) electric detonator, 2) explosive charge, 3) powder packing, 4) regulating support, 5) obstacle.

Some Initial Conditions of Superdeep Penetration which Follow from the Necessary and Sufficient Conditions. The above necessary (1) and sufficient (8) conditions of superdeep penetration make it possible to determine a number of the important characteristics of this process. For example, when the particle size is fixed, from (1) one can determine the minimum velocity of the particles at which superdeep penetration is still possible:

$$U_{\mathrm{p}} \geq U_{\min} = \frac{ad}{\Delta^2}, \tag{9}$$

which will be $U_{\min} \approx 315$ m/sec for iron at $\Delta = 1.5 \cdot 10^{-6}$ m, $d \approx 55 \cdot 10^{-6}$ m, $\rho = 7830$ kg/m^3 [9], and $a = 1.29 \cdot 10^{-5}$ m^2/sec. It follows from conditions (8) and (1) that the inequalities $U_{\min} \leq U_{\mathrm{p}} \leq U_{\max}$ must always hold for the velocity of the penetrating particle. This means that, at least, $U_{\min} \leq U_{\max}$. Whence we calculate the threshold (critical) pressure in the obstacle, i.e., the minimum pressure necessary for realization of superdeep penetration:

$$\frac{ad}{\Delta^2} \leq \sqrt{\frac{p}{\rho}} \quad \text{or} \quad p \geq p_{\mathrm{cr}} = \frac{\rho a^2 d^2}{\Delta^4}. \tag{10}$$

In our case (steel obstacle) we have $p_{\mathrm{cr}} \approx 0.78$ GPa. Conditions (8) and (9) obtained for the first time in [13] determine the narrow "corridor" of the particle velocities at which superdeep penetration is possible. In the calculations with the use of (9) we are dealing with the velocity with which a particle comes to the surface of the obstacle, while (8) determines the maximum velocity of a particle retarded in the near-surface obstacle layers, where the superdeep-penetration mechanism does not act. According to the conclusions drawn in [13], by the time the superdeep-penetration mechanism begins to act the velocity of the particle must be

$$V_{\mathrm{p}} = \sqrt{U_0 \exp(-Z) - \frac{p}{\rho}(1 - \exp(-Z))}, \tag{11}$$

where

$$Z = \frac{\rho S d}{M}. \tag{12}$$

Parameters of the Gas-Powder Flux Accelerated by an Explosive Accelerator. Superdeep Penetration. Further development of the superdeep-penetration model is impossible without determining the gas-powder flux gener-

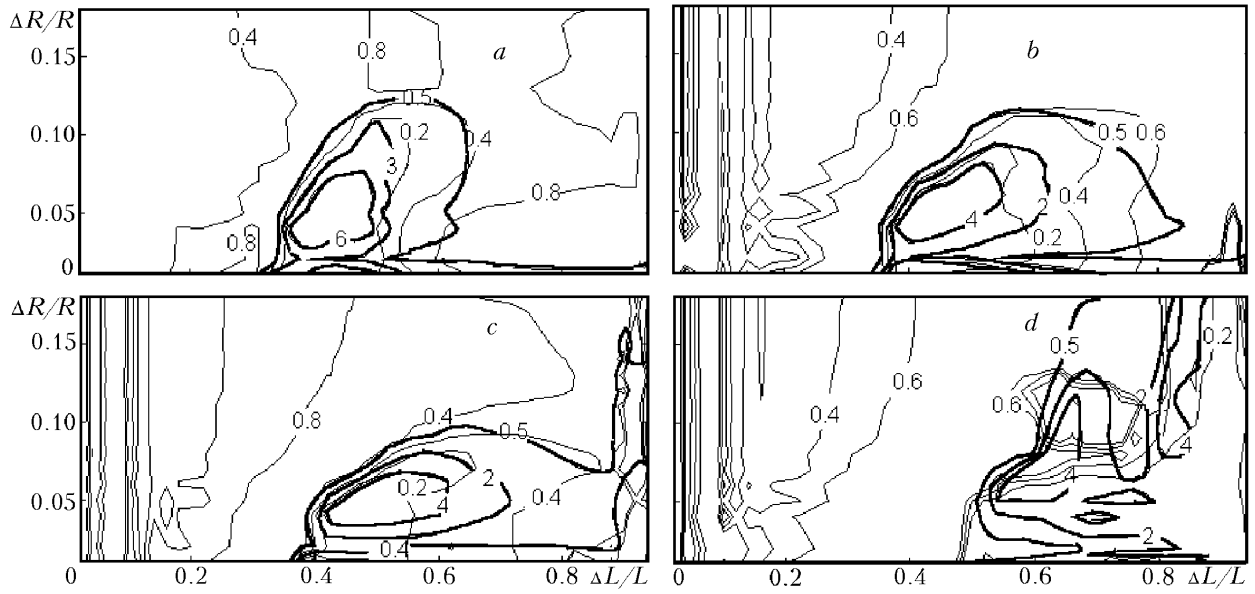

Fig. 2. Isolines of the density (semiboldface curves) and the velocity (thin curves) of the flow generated by the explosive accelerator: a) t = 50, b) 75, c) 100, and d) 150 μsec.

ated by an axially symmetric accelerator with a conical recess (Fig. 1). This generator was used in [14–17] for acceleration of the particles of stannic (electrolytic)-bronze powder. The particle flux was modeled numerically [3, 15, 16]. The calculations carried out made it possible to obtain the characteristics of the flux in the form of isolines of the basic hydrodynamic parameters (Fig. 2). Figure 2a shows the isolines of the density (semiboldface lines) and the longitudinal velocity (thin lines) of the flux at the initial period of its interaction with the obstacle (t = 50 μsec and L = 0.11 m; a unit of density corresponds to 1000 kg/m^3 and a unit of velocity corresponds to 4000 m/sec). The time is measured from the beginning of the detonation of the explosive charge; in our case, the explosive is 6ZhV ammonite. A thin high-velocity jet (Fig. 2a) propagating along the axial line with a velocity of the order of 0.75D is clearly defined. For 6ZhV ammonite, $D \approx 4000$ m/sec at the initial density ρ_e = 1000 kg/m^3. The density of the jet is initially low ($\rho_0 \approx$ 300–400 kg/m^3). At t = 75 μsec, the velocity of the jet markedly decreases while its density slightly increases (Fig. 2b). By the instant of time t = 100 μsec, the major part of the flux comes to the surface of the obstacle (Fig. 2c) and the rate of interaction decreases constantly, whereas the density of the flux increases constantly. By the time t = 150 μsec, the interaction occurs at a very small velocity (~300 m/sec) and by $t \approx 169$ μsec it stops completely. The integral change in the hydrodynamical parameters of the gas-powder flux with time is presented in Fig. 3a and b. The number of particles interacting with the obstacle per unit time throughout the interaction cross section σ_{int} is equal to

$$N = \rho_0 U_0 \sigma_{int} . \tag{13}$$

The dependence of N on the loading time t for our concrete case is given in Fig. 3c. The total number of the particles interacting with the obstacle during the time interval from t to $t + \Delta t$ is determined as

$$n = \int_t^{t+\Delta t} N(\Theta)\, d\Theta . \tag{14}$$

However, the number of particles obtained from formula (14) will always be overstated. This is because the model developed in [3, 15, 16] cannot in essence describe the collisional interactions in the flux and gives no way of taking into account the process of sticking of particles to the surface of the obstacle and the process of blocking which accompanies the interaction and at which the obstacle surface is screened by a cloud of particles reflected from it. Ac-

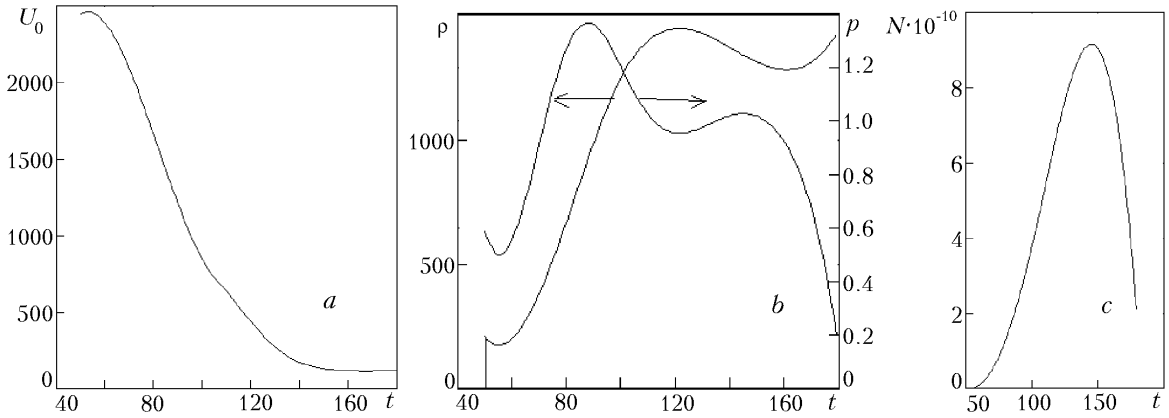

Fig. 3. Dependences of the longitudinal velocity of the flux U_0 (a), its density ρ and pressure p (b), and the number of particles in the cross section of interaction of the flux with the obstacle per unit time N (c) on the loading time. t, μsec; U_0, m/sec; ρ, kg/m^3; p, GPa; N, 1/sec.

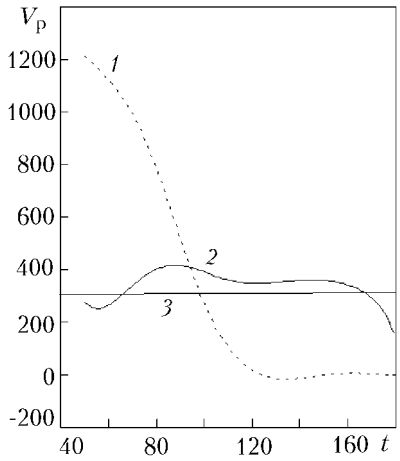

Fig. 4. Velocity curves for steel loaded by a particle flux: 1) U_p, 2) U_{max}; 3) U_{min}. V_p, m/sec; t, μsec.

cording to [16, 17], as a result of this inevitable loss, less than 10% of the particles coming to the surface of the obstacle can interact with it. Figure 4 shows a fairly exact pattern of the penetration. From the beginning of the interaction up to the first intersection of curve 2 and the straight line 3 in Fig. 4, superdeep penetration is impossible since the pressure generated in the obstacle by the particle flux is lower than the critical pressure. From the instant of the first intersection of curves 2 and 3 to the intersection of curves 1 and 2 the velocity V_p is higher than the velocity U_{max}. In this interval, the velocity of the particles is too high for superdeep penetration, the channel behind the particle closes incompletely, and the drag force is nonzero. The velocity of the particles begins to rapidly decrease until it is equal to U_{max}, whereupon the object moves in the material with a given velocity uniformly and rectilinearly unless it is confronted by inhomogeneities or inclusions contained in the actual material of the obstacle. The interactions with these barriers can substantially decrease the velocity of a penetrating object and change the direction of its movement. The particles interacting with the obstacle from the instant of time corresponding to the intersection of curves 1 and 2 up to the intersection of curves 1 and 3 (Fig. 4) move with a velocity $U_{min} \le V_p \le U_{max}$. All the particles that came to the obstacle at a later time (Fig. 4) have a velocity $V_p < U_{min}$ and are incapable of penetrating, since the necessary condition of superdeep penetration is not observed for them. However, the process of movement of particles that began to move to the obstacle earlier can occur up to the instant of time corresponding to the second intersection of curves 2 and 3. At this point, the pressure becomes lower than the critical pressure once again and superdeep penetration becomes impossible. A numerical approximation of the above-described dependences allows one to calculate the number

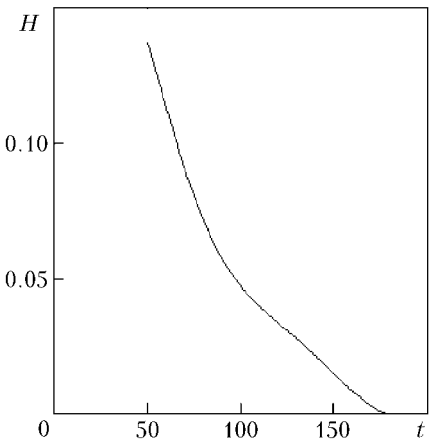

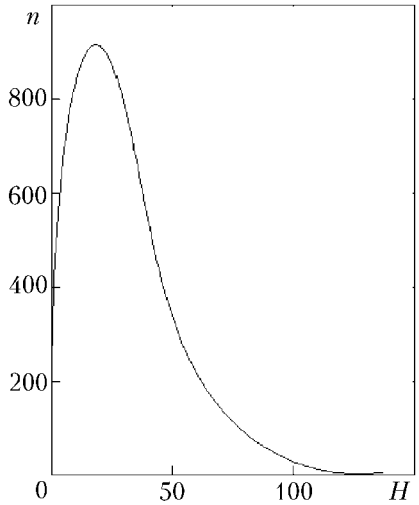

Fig. 5. Dependence of the depth of penetration of particles H on the loading time t. H, m; t, μsec.

Fig. 6. Distribution of particles n over the penetration depth H. H, mm.

of particles participating in the process of penetration at each its stage. Let us denote the beginning and the end of the process of loading of the obstacle by a gas-powder flux by t_{00} and t_{fin}, the instants of time corresponding to the intersections of curves 1 and 2 and 1 and 3 by t_{12} and t_{13}, and the instants of time corresponding to the first intersection of curves 2 and 3 by t_{23} and to the second intersection of curves 2 and 3 by t_{32}. The total number of particles participating in the interaction will be equal to

$$N_{\text{int}} = \int_{t_{00}}^{t_{\text{fin}}} N(\Theta)\, d\Theta\,, \tag{15}$$

and the number of particles penetrating by the mechanism of superdeep penetration will be

$$N_{\text{SDP}} = \int_{t_{23}}^{t_{12}} N(\Theta)\, d\Theta + \int_{t_{12}}^{t_{13}} N(\Theta)\, d\Theta\,. \tag{16}$$

The integral in (16) is divided into two parts to underscore that the fraction of particles determined by the second integral in (16) participates in superdeep penetration if the necessary and sufficient conditions of superdeep penetration are accurately observed. The first integral of equality (16) corresponds to the part of the flux in which a uniform penetration is preceded by the stage of slow motion. Let us denote these numbers of particles by N_{23} and N_{12} respectively. The fraction of the penetrating particles of the flux can be determined as

$$\delta_{\text{SDP}} = \frac{N_{\text{SDP}}}{N_{\text{int}}} = \frac{N_{23}}{N_{\text{int}}} + \frac{N_{12}}{N_{\text{int}}} = \delta_{12} + \delta_{23}\,. \tag{17}$$

From the results of the numerical investigations, $\delta_{23} \approx 0.0065$ and $\delta_{12} \approx 0.0021$. In this case, less than one percent of the particles coming to the obstacle participate in the process of superdeep penetration. Here, account is taken of the fact that, because of the blocking and sticking processes, less than 10% of all the particles coming to the obstacle interact with it. At the same time, as is seen from Fig. 4, the highest-velocity part of the particle flux, equal to

$$\delta_{\text{out}} = N_{\text{int}}^{-1} \int_{t_{00}}^{t_{23}} N(\Theta)\, d\Theta\,, \tag{18}$$

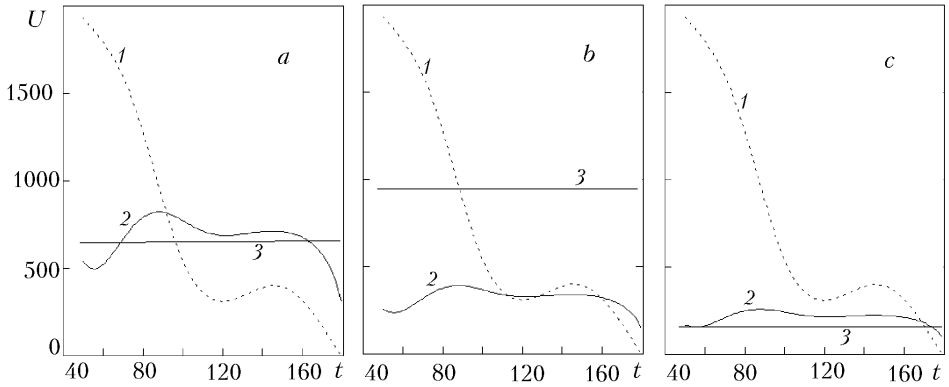

Fig. 7. Velocity curves for aluminum (a), silver (b), and lead (c): 1) V_p; 2) U_{max}; 3) U_{min}. U_p, m/sec; t, μsec.

does not participate in superdeep penetration, since the pressure in the obstacle is much lower than the critical pressure. In this case, $\delta_{out} \approx 0.003$. The total number of particles in a packing can also be determined if the weight of the packing m and the weight of one particle M are known. If the assumption is made that the strikers are spherical,

$$M = \rho_p \frac{\pi d^3}{6}, \tag{19}$$

the total number of particles in the packing will be

$$N_{tot} = \frac{m}{M}. \tag{20}$$

When an accelerator is used (Fig. 1), we have $m \approx 0.011$ g, diameter of the bronze particles d = 55 μm, $N_{tot} \approx 1.419 \cdot 10^7$, and $N_{int} \approx 6.156 \cdot 10^6$ particles interacting with the obstacle if the blocking is disregarded. Thus, taking into account the blocking processes, we obtain $N_{12} \approx 1290$ and $N_{23} \approx 3290$, which is quite consistent in order of magnitude with the experimental data of [15–17]. Figure 5 shows the dependence of the depth of penetration of particles on the interaction time. As was to be expected, this dependence is close to the linear dependence. The interaction time also determines the position of the particle in the flux interacting with the obstacle surface. The distribution of the particles over the depth is presented in Fig. 6. The curve $n(H)$ has a pronounced maximum at a depth of 17–18 mm. The limiting depth of penetration into the obstacle is expressed by the formula

$$H_{max} = \int_{t_{23}}^{t_{32}} U_{max}(\Theta)\, d\Theta = \int_{t_{23}}^{t_{32}} \sqrt{\frac{p(\Theta)}{\rho}}\, d\Theta \tag{21}$$

and is 71 mm for steel. Unfortunately, the details of the process of interaction of a particle with the obstacle material have not been adequately investigated and the experimental data on the change in the mass and size of the particle as a result of the penetration can be found only in [14, 16, 17]. Therefore, a more detailed modeling of superdeep penetration with determination of the mass flow through each cross section and the dependence of the concentration of the introduced material on the penetration depth seems to be impossible at present. However, the above-described model enables us to determine the character of the penetration of particles into different materials. To do this we must obtain curves analogous to those presented in Fig. 4 for steel for other metals as well. As is seen from Fig. 7a, the process of penetration of a particle flux generated by an accelerator into aluminum (Fig. 1) is similar in general terms to the process of superdeep penetration of this flux into steel, while in silver (Fig. 7b) such penetration is impossible since the background pressure remains invariably lower than the critical pressure. The penetration into lead proceeds most actively (Fig. 7c) since the major part of the flow is working. Practically everywhere it proceeds with a velocity U_{max}. But since the pressure generated in the obstacle by the particle flux is very low in lead and the velocity is

$U_{max} \sim 100$–220 m/sec, the limiting penetration depth H_{max} determined from (21) is small in comparison with the depth of penetration into aluminum or steel. In our case, we have $H_{max} \approx 16$ mm for lead, whereas we have $H_{max} \approx 98$ mm for aluminum and $H_{max} \approx 71$ mm for steel.

CONCLUSIONS

As the investigations carried out have shown, the process of superdeep penetration occurs when two basic conditions are fulfilled. The condition necessary for realization of superdeep penetration is a thermoplastic softening of the obstacle material in the local region immediately adjacent to the penetrating particle. The sufficient condition for superdeep penetration is a rapid closing of the channel behind the particle under the action of the pressure generated in the obstacle by the particle flux interacting with it. If this closing is quite rapid and the wake (channel in our case) formed by the particle in the obstacle material closes completely, the penetrating particle moves in the obstacle material without meeting resistance. An analog of the D'Alembert paradox [11] which, in the classical understanding, is characteristic of a perfect fluid is realized. In our case, its realization becomes possible due to the external energy source (particle flux) which does work providing a complete closing of the channel in the wake of the penetrating particles, which allows them to move in the obstacle material without meeting resistance. The numerical model of gas-powder flow, proposed in [14, 15], makes it possible to calculate the most important characteristics of superdeep penetration (limiting depth, velocity of penetration, fraction of penetrating particle) and to determine the character of the process. However, to describe superdeep penetration exhaustively, it is necessary to investigate the character of interaction of particles with the incoming flux of the softened obstacle material in more detail and to find the dependences describing the change in the size and mass of the particles in the process of their penetration deep into the obstacle.

The author is grateful to V. A. Shilkin for his participation in the discussion of the results, R. I. Shit' for his personal assistance in the work, and G. S. Romanov for constant support and participation in the discussion of the results of the investigations.

NOTATION

U_0, velocity of the flux particles at the level of the obstacle surface, m/sec; p, pressure generated in the obstacle by the particle flux, Pa; m, weight of the powder packing in the accelerator, kg; U, velocity of stationary flow of the softened-material flux around a particle, m/sec; v, local velocity of the fluid in the wake, m/sec; V_p, velocity of a particle after the penetration to the depth $h = d$, m/sec; D, detonation rate of the explosive, m/sec; h and H, running and final depth of penetration of a particle, m; M, d, and S, mass, diameter, and midsection of the particle, kg, m, and m^2; ρ and ρ_p, densities of the obstacle and of the particle, kg/m^3; τ_{int}, characteristic time of interaction, sec; τ_{cl}, time of complete closing of the channel formed by a particle, sec; r and u, radial coordinate and velocity component of the obstacle material, m and m/sec; ΔS, cross-sectional area of the channel (wake), m^2; t, running time of loading, μsec; Z, dimensionless parameter characterizing the penetration depth; T and a, temperature and thermal diffusivity of the obstacle, K and m^2/sec; Δ, thickness of the slip planes of the obstacle, m; p_{cr}, minimum threshold pressure of superdeep penetration, Pa; x, coordinate in the direction of particle motion; z and y, coordinates perpendicular to x; δ, fraction of the flux particles; F_x, drag force acting on the penetrating particle from the obstacle, N; n and N, distribution of particles and their number in the interaction cross section; σ, cross section of interaction of the particle flux with the obstacle, m^2; Δt, physically small time interval; Θ, integration variable; R and L, radius and length of the accelerated particle. Subscripts: min, minimum; max, maximum; int, interaction parameter; th, thermal parameter; cl, parameter of filling (closing) of the channel; fin, parameter of completion of the process; 0, value of the parameter in the particle flux; 00, initial value; p, parameters of the particle; e, parameters of the explosive; tot, total number of particles; out, high-velocity part of the flux which does not participate in the penetration; cr, critical; lim, limiting; SDP, superdeep penetration.

REFERENCES

1. L. V. Al'tshuler, S. K. Andilevko, G. S. Romanov, and S. M. Usherenko, *Pis'ma Zh. Tekh. Fiz.*, **15**, Issue 5, 55–57 (1989).

2. L. V. Al'tshuler, S. K. Andilevko, G. S. Romanov, and S. M. Usherenko, *Inzh.-Fiz. Zh.*, **61**, No. 1, 41–45 (1991).
3. S. K. Andilevko, *Superdeep Mass Transfer of Discrete Microparticles in Metal Obstacles under the Conditions of Loading the Latter by a Powder Flux*, Candidate's Dissertation (in Physics and Mathematics), Minsk (1991).
4. S. K. Andilevko, *Inzh.-Fiz. Zh.*, **71**, No. 3, 399–403 (1998).
5. S. K. Andilevko, *Int. J. Heat Mass Transfer*, **41**, Nos. 6–7, 957–962 (1998).
6. S. K. Andilevko, S. S. Karpenko, and O. V. Roman, *Inzh.-Fiz. Zh.*, **73**, No. 5, 1050–1055 (2000).
7. G. G. Chernyi, *Dokl. Akad. Nauk SSSR*, **292**, No. 6, 1324–1328 (1987).
8. S. M. Usherenko, *Inzh.-Fiz. Zh.*, **75**, No. 3, 183–198 (2002).
9. S. P. Kiselev and V. P. Kiselev, *Prikl. Mekh. Tekh. Fiz.*, **41**, No. 2, 37–44 (2000).
10. O. V. Roman, S. K. Andilevko, S. S. Karpenko, G. S. Romanov, and V. A. Shilkin, *Inzh.-Fiz. Zh.*, **75**, No. 4, 187–197 (2002).
11. L. D. Landau and E. M. Lifshits, *Hydrodynamics* [in Russian], Moscow (1986).
12. L. I. Sedov, *Continuum Mechanics* [in Russian], Vol. 1, Moscow (1984).
13. S. K. Andilevko, *Inzh.-Fiz. Zh.*, **75**, No. 5, 47–50 (2002).
14. O. V. Roman, S. K. Andilevko, and S. S. Karpenko, *Scientific Report* No. 19992123, Minsk (1999).
15. S. K. Andilevko, O. A. Dybov, and O. V. Roman, *Inzh.-Fiz. Zh.*, **73**, No. 4, 797–801 (2000).
16. S. K. Andilevko, S. S. Karpenko, and O. V. Roman, *Inzh.-Fiz. Zh.*, **74**, No. 1, 73–78 (2001).
17. O. V. Roman, S. K. Andilevko, and S. S. Karpenko, *Zh. Khim. Fiz.*, **21**, No. 9, 50–54 (2002).